Multiple Resonant Frequency Offset Acquisitions for Imaging of Metallic Implants

K. M. Koch[1], R. F. Busse[2], T. A. Lewein[1], H. G. Potter[3], R. S. Hinks[1], and K. F. King[1]

[1]Applied Science Laboratory, GE Healthcare, Waukesha, WI, United States, [2]Applied Science Laboratory, GE Healthcare, Madison, WI, United States, [3]Magnetic Resonance Imaging, Hospital for Special Surgery, New York, NY, United States

Introduction: It has previously been demonstrated that MRI has utility in diagnosing complications from arthroplasty [1,2]. Unfortunately, B_0 field perturbations generated by most prosthetic material compositions produce unacceptable spatial distortions in conventional MR images. Unconventional imaging methods such as single-point imaging [3], pre-polarized MRI [4], and view-angle tilting (VAT) [5] have been proposed and demonstrated to reduce the impact of the implant-induced image distortions. Of these approaches, only VAT has been demonstrated in a clinical environment [6]. VAT is inherently a 2D technique, and while it can mitigate in-plane distortions, it suffers from residual distortion in the slice-select dimension. To reduce this effect, a field-map based correction has been proposed [7].

Theory: Here, an alternative method utilizing 3D MRI techniques to mitigate implant-induced artifacts is presented. A single on-resonance 3D MR acquisition will possess significant signal voids in the vicinity of metal implants (see Figure 1B). Such voids result from proton resonance frequencies near the implant being outside the frequency band of RF pulses. Furthermore, even if RF pulses of infinite bandwidth were hypothetically applied, the resulting ΔB_0-induced readout distortions would severely limit the diagnostic quality of resulting images.

To address both of these artifact considerations, the presented method collects multiple 3D fast-spin-echo (FSE) images at discretely stepped resonance frequency (transmitted and detected) offsets. By utilizing resonance-offset intervals, $\Delta\omega_0$, that are within the bandwidth of the RF pulses, a complete composite image can be created from the individual reconstructed images. In this demonstration, a maximum intensity projection (MIP) combination process is utilized.

A crucial property of the presented method is that the maximum effective ΔB_0 for spins being collected in a single image is $\Delta\omega_R/2$, where $\Delta\omega_R$ is the bandwidth of the RF pulses. This is a consequence of moving both the transmission and detection center frequency synchronously. This enables the collection of individual images (and combined composite images) with greatly reduced readout distortions limited to $\Delta n_{max} = N*\Delta\omega_R/(2*RBW)$, where Δn is a pixel shift and N is the total number of readout samples. For example, when using RF pulses with a bandwidth of 2kHz with a 256-sample readout of bandwidth of +/-125kHz, the maximum readout distortion is roughly 2 pixels, *for any off-resonance spin*. In comparison, a conventional 2D FSE image will possess far more readout distortion due to the use of frequency-offset RF pulses *without* synchronous offsets in central readout and transmission frequencies.

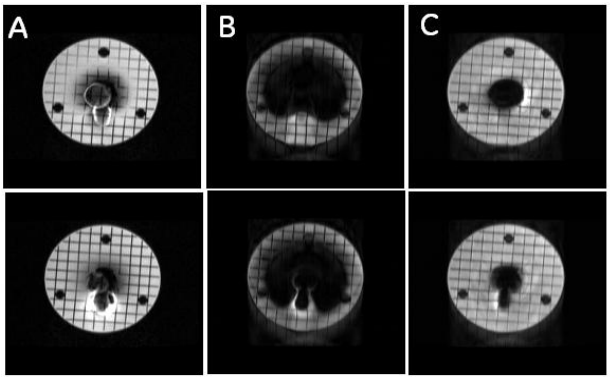

Figure 1: A) 2D FSE images, B) on-resonance ($\Delta\omega_0 = 0$) single 3D images, and C) composite 3D images near the cobalt-chromium femoral head component of a total hip replacement phantom.

Methods: Imaging experiments were performed on a GE Signa 1.5T scanner. Images were collected cobalt-chromium titanium based total hip (phantom) and knee (*in vivo*) replacement prostheses. Composite images were computed from 28 individual axial 3D FSE images using non-selective (i.e. no slab-selection gradients were applied) Shinnar-LeRoux (SLR) excitation and refocusing pulses (bandwidth = 2.3 kHz) with frequency shifts of 0.75 kHz (spanning roughly +/- 10 kHz). Images were collected with a 256 x 128 x 56 data matrix over 27 x 21 x 28 cm, TE = 35 ms, TR = 350 ms, readout bandwidth (RBW) of +/- 125 kHz, and an echo-train-length (ETL) of 32. For comparison purposes, 2D FSE images with 1.2 kHz SLR excitation and refocusing pulses were acquired over the identical geometry with the same TE, TR, ETL, and RBW settings. The total scan times for the two image acquisitions were 4.25 min for the 2D FSE image and 40 min for the 3D composite image.

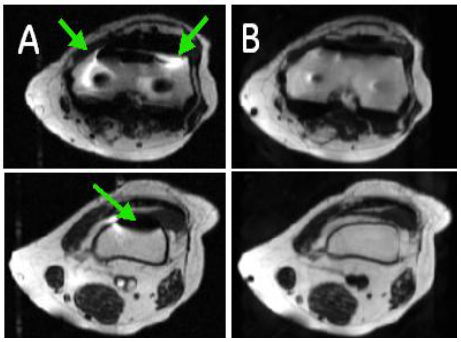

Figure 2: Axial A) 2D FSE images and B) composite 3D images of a volunteer with a total knee replacement prosthesis. Green arrows indicate artifact-prone regions (near cobalt-chromium femoral component) that are repaired in the composite image.

Results and Discussion: Figure 1 shows results phantom experiment results. There are significant object formation differences in the 2D (A) and 3D composite images (C) for identical *physical slice locations*. This largely due to off-resonance spin-density mis-registrations in the slice-direction for spins near the implant. The on-resonance 3D image (B) shows the dramatic effect of the implant-induced B_0 distribution on RF spatial selectivity. The 3D composite image possesses no slice-direction distortion and reduced readout distortion. In the near vicinity of the implant, the 2D images possess severely compromised diagnostic information, whereas the 3D composite images clearly enable increased MR imaging access to these regions. The residual localized intensity pileups the composite 3D images result from local field gradients overcoming the readout encoding gradient strength and are likely dominated by nearest-neighbor pixel interactions. *In vivo* images of a total-knee implant are provided in Figure 2. Green arrows indicate regions with the most dramatic artifacts in the 2D images (A), which are largely removed in the 3D composite images (B). Again, there are noticeable variations in structural formation between images (A-B) for identical physical slice locations.

Future work will focus on developing more advantageous frequency windowing strategies (both RF pulse-shapes and frequency offsets) along with reducing the total acquisition times. Because individual image acquisitions interact with independent spin ensembles, the method lends itself to an interleaved acquisition strategy. Such interleaving will enable reduced ETL acquisitions (and higher fidelity images) in less overall acquisition time as well as increased flexibility in TE/TR ratios. Partial k-space, zero filling, compressed sensing, and parallel imaging techniques will also be explored to further reduce scan time. Initial estimates and calculations suggest that with such acceleration strategies, high-resolution clinically viable composite 3D images may be viable with less than 15-minute scan-times. Further investigations will also explore iterative reconstruction strategies that may enable removal of intensity pileups in regions where the local inhomogeneity gradient supersedes the magnitude of the readout-encoding gradient.

[1] HG Potter, et al. Clin Orthop. 1995 **319**:223–31.

[2] HG Potter, et al. J. Bone Joint Surg. Am., 2004 **86-A**(9): 1947-54

[3] P Ramos-Cabrer, et al., MRI. 2004 **22**: 1097-1103

[4] RD Venook et al., MRM. 2006 **56**: 177-186

[5] ZH Cho et al., Med. Phys. 1988 **15**(1): 7-11.

[6] K Butts., JMRI. 1999 **9**: 586-595.

[7] K Butts et al., Proc. ISMRM. 2006. 2380.